Development of Multi-Strip Image Mosaicking for KOMPSAT-3A Images

Jong-Hwan Son [1], Sumin Park [2], Hyeon-Ju Ban [3], Taejung Kim [4]

[1] Image Engineering Research Center, 3DLabs Co., Ltd., Incheon, Republic of Korea – json8520@3dlabs.co.kr
[2] Satellite Application Division, Korea Aerospace Research Institute, Daejeon, Republic of Korea – smpark113@kari.re.kr
[3] Satellite Application Division, Korea Aerospace Research Institute, Daejeon, Republic of Korea – hjban@kari.re.kr
[4] Dept. of Geoinformatic Engineering, Inha University, Incheon, Korea – tezid@inha.ac.kr

Keywords: Image Mosaicking, Seamline Extraction, Image Matching, Relative Geometric Correction, KOMPSAT-3A.

Abstract

High-resolution satellite imagery has a limitation in terms of coverage area. This limitation presents challenges for extensive-scale analysis at regional or national levels. To maximize the utility of high-resolution satellite imagery, the implementation of image mosaicking techniques is essential. In this paper, we have developed seamline extraction techniques and relative geometric correction optimized for high-resolution satellite imagery. Ultimately, we proposed a multi-strip image mosaicking method for KOMPSAT-3A(Korea Multi-Purpose Satellite-3A) images. We applied the Dijkstra's shortest path algorithm to efficiently extract seamlines. we also performed image registration based on feature matching and homography transformation to correct the relative geometric errors between input images. We conducted experiments with our methods using 29 scenes from KOMPSAT-3A L1G data. The results indicated high relative geometric accuracy, with an average error of 1.63 pixels. Furthermore, we were able to obtain high-quality seamless mosaic images. Our proposed method is expected to enhance the utility of KOMPSAT-3A imagery for large-scale environmental and urban analysis and to provide more accurate and comprehensive data.

1. Introduction

In recent years, satellite imagery has seen rapid advancements in spatial resolution, greatly expanding its applicability in various fields. Today's high-resolution images, surpassing the limited information provided by early satellite images, can capture the Earth's surface with unprecedented detail. This improvement allows for a more accurate and comprehensive understanding of geographical features, thereby fundamentally transforming approaches in environmental monitoring, urban planning, and other critical studies.

However, despite offering detailed observations, high-resolution satellite imagery has a limitation in terms of coverage area, particularly when compared to medium or low-resolution imagery. This limitation presents challenges for extensive-scale analysis at regional or national levels. Moreover, due to the orbital paths of satellites, an entire area of interest may not be captured in a single path. Therefore, to maximize the utility of high-resolution satellite imagery, the implementation of image mosaicking techniques is essential. Image mosaicking has to ensure comprehensive analysis over the entire region of interest by combining multiple images into one large image.

To address the challenge of limited coverage in high-resolution satellite imagery, numerous studies have been conducted within remote sensing and satellite imagery analysis community. In initial studies, image mosaicking was performed by aligning images based on common control points (Milgram, 1975; Shiren et al., 1989; Afek and Brand, 1998). Milgram (1975) focused on extracting control points that minimized the differences between pixel values along image lines, facilitating image mosaicking based on these common control points. Afek and Brand (1998) introduced a mosaicking method that utilized tie-points derived from stereo image matching. Although effective to a degree, these methods often resulted in geometric distortions and mismatches, particularly in some non-control point areas.

Recently, many studies have focused on extracting seamline by analyzing the relationships among image information in overlapping areas and to minimize geometric distortions and mismatches (Li et al., 2018; Zhang et al., 2018; Yuan et al., 2020). Li et al. (2018) constructed image energy map using gradient and edge segmentation information and extracted seamline based on graph cut algorithm. Zhang et al. (2018) presented a method for optimizing seamline detection in urban aerial image mosaicking using graph cuts. Their technique combined data from Digital Surface Models (DSM) with image color and gradient information to extract seamline, avoiding buildings. Yuan et al. (2020) introduced a method for seamline detection in urban mosaics using D-LinkNet to generate road probability maps, guiding seamlines along roads to minimize visual disruptions and improve mosaicking quality.

Recent studies have presented image mosaicking methods that significantly reduce geometric distortions and mismatches. However, there remains a limitation that the relative geometric error between the input images must be nonexistent or negligible. Relative geometric errors between satellite images are inevitably present, attributable to factors such as variations in payload position and attitude, sensor distortion errors, and the effects of Earth's curvature and rotation (Kim et al., 2007; Kim et al., 2018). Furthermore, the problem of relative geometric errors becomes increasingly pronounced as the number of satellite images used for mosaicking increases. Therefore, the development of multi-image mosaicking techniques that consider relative geometric correction between satellite images is necessary.

In this paper, we proposes a multi-strip image mosaicking method for KOMPSAT-3A(Korea Multi-Purpose Satellite-3A) images. we have developed a seamline extraction and relative geometric correction technique suitable for high-resolution satellite imagery and performed mosaicking based on multi-strips to minimize geometric errors between images. This proposed method is expected to enhance the utility of KOMPSAT-3A imagery for large-scale environmental and urban analysis and to provide more accurate and comprehensive data.

2. Methodology

In order to acquire high-quality mosaic images, it is important to extract seamlines that minimize the disparity in the mosaic image and to correct relative geometric errors between input images. Therefore, in this study, we have developed seamline extraction techniques and relative geometric correction optimized for high-resolution satellite imagery. we propose a multi-strip image mosaicking method that applies these developed techniques to achieve a seamless and cohesive final mosaic image.

2.1 Seamline Extraction

Extracting the optimal seamline is necessary for achieving a seamless mosaic in high-resolution satellite imagery, where numerous objects are identifiable in detail (Li et al., 2019; Zagrouba et al., 2009). To efficiently extract seamlines in high-resolution satellite images, we apply the Dijkstra's shortest path algorithm. This algorithm calculates the shortest path between the vertices in a graph, considering the weight of each edge (Dijkstra, 1959). To extract the seamline based on the Dijkstra's algorithm, we analyze the overlap between satellite images and constructed a graph structure. Weights are determined based on the image gradient. Finally, we adjust the Dijkstra's algorithm to calculate the shortest path, which is used as the seamline.

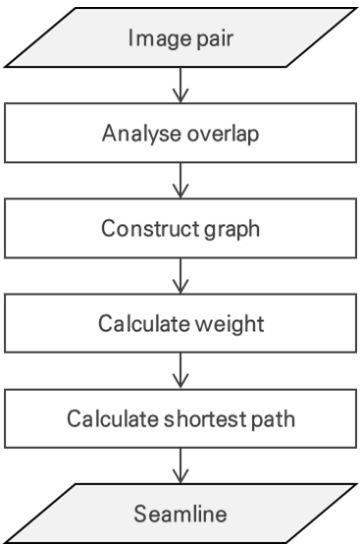

Figure 1. Workflow of seamline extraction

2.1.1 Analyse Overlap: To define the area for seamline extraction and construct the graph, we first perform an analysis of the overlapping areas between satellite images. Based on the relative geometry between satellite images, the overlapping areas are calculated. The intersection points of the satellite image contours are determined, and from these, the two points farthest apart are identified to define the start and end vertex of the seamline. The extraction direction of the seamline is then determined by comparing the column and row differences between these points. If the column difference is greater, the seamline extraction direction is set horizontally; if the row difference is greater, it is set vertically.

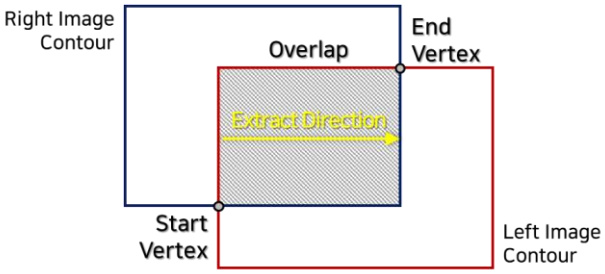

Figure 2. analysis of overlap between satellite images

2.1.2 Construct Graph: To analyze the relationships between pixels in the overlapping area, we transform the image array of the overlapping area into a graph structure. Each pixel in the image is defined as a vertex, and the directed lines between vertices are defined as edges. These edges are constructed unidirectionally from the upper vertex to the lower vertex based on the seamline extraction direction. As the number of edges connecting from the upper row to the lower row increases, the complexity of the graph increases. If the graph's complexity is too low, the relationships between pixels are inadequately considered, resulting in a low-quality seamline. Conversely, if the complexity is too high, it leads to excessive processing time. to maintain optimal graph complexity for high-resolution satellite image seamline extraction, the number of edges is limited to a maximum of 15 on each side, based on the position of the upper vertex.

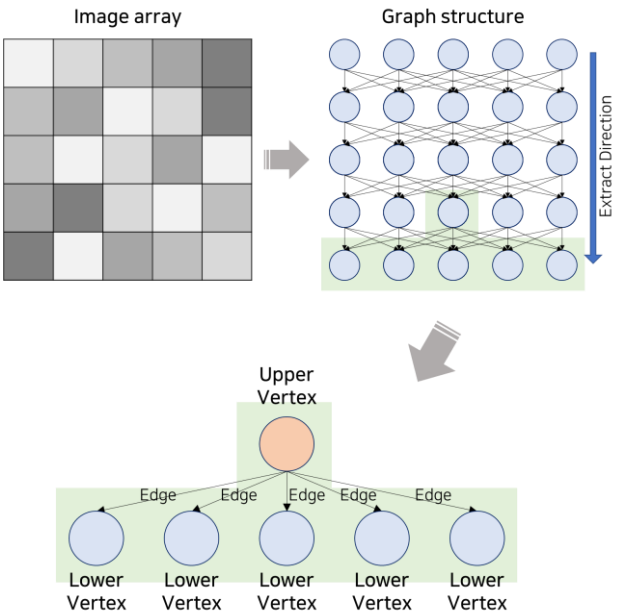

Figure 3. Example of graph construction

2.1.3 Calculate Weight: To generate seamless mosaic image, the seamline must be positioned to minimize the intensity and geometric differences between images (Duplaquet, 1998). Therefore, we calculate the weights based on differences in pixel values and gradients between the satellite images. Since differences between input images exist in horizontal and vertical directions, we divide the weights into two types of costs: horizontal cost(HC) and vertical cost(VC). HC is calculated from pixel value and gradient differences with the previous vertex, while VC uses differences with the vertex below. The detailed equations are as follows.

$$HC(i,j) = \frac{(f(i,j)-g(i-1,j))^2 + (f(i-1,j)-g(i,j))^2}{2(\Delta f(i,j) + \Delta f(i-1,j) + \Delta g(i,j) + \Delta g(i-1,j)+1)}$$

$$VC(i,j) = \frac{(f(i,j)-g(i,j+1))^2 + (f(i,j+1)-g(i,j))^2}{2(\Delta f(i,j) + \Delta f(i,j+1) + \Delta g(i,j) + \Delta g(i,j+1)+1)}$$

where f(i,j), g(i,j) = pixel value at column *i* and row *j*
Δf(i,j), Δg(i,j) = gradient value at column *i* and row *j*
HC(i,j) = horizontal cost of vertex at column i and row j
VC(i,j) = vertical cost of vertex at column i and row j

Ultimately, the weight is calculated as the sum of a single cross-extract direction cost and the cumulative extract direction cost. As the distance between the upper and lower vertices increases, the cumulative extract direction cost also rises, which helps to minimize excessive fluctuations in the seamline.

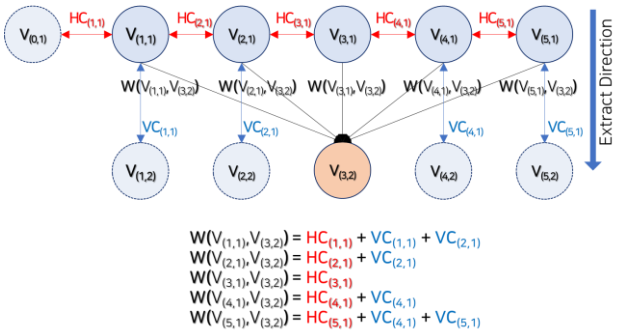

Figure 4. Example of weight Calculation

2.1.4 Calculate shortest path: We calculate the shortest path connecting the start and end vertices in the constructed graph using the Dijkstra's algorithm. Since this path is at the position that minimizes the differences between the images in the overlapping area, it is assumed to be the optimal seamline.

2.2 Relative Geometric Correction

To correct the relative geometric errors between the target and reference images, we perform feature matching to extract tie-points. We then improve the accuracy of these tie-points by eliminating outliers. Based on these tie-points, we estimate the transformation model between the input images and resample the target image to align it with the reference image.

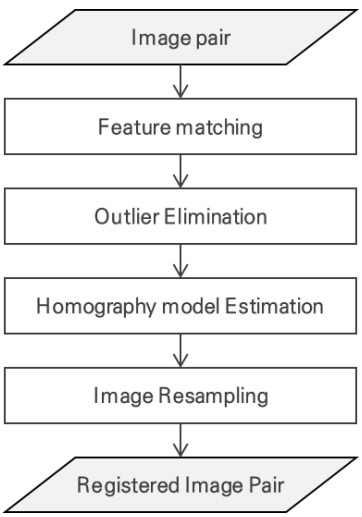

Figure 5. workflow of relative geometric correction

2.2.1 Feature Matching: we perform feature matching based on the SIFT(Scale-Invariant Feature Transform). SIFT is an algorithm for extracting and matching feature points in images, capable of identifying consistent features across various scales and rotations, and demonstrates high performance in feature matching (Lowe, 2004; Wu et al., 2013). In typical brute-force based feature matching, each feature of the target image is matched against all features of the reference image. In this study, we impose constraints on the search range for each feature, based on the geometric information of the satellite images. This approach significantly reduce the number of matching candidates for each feature, leading to improved feature matching performance.

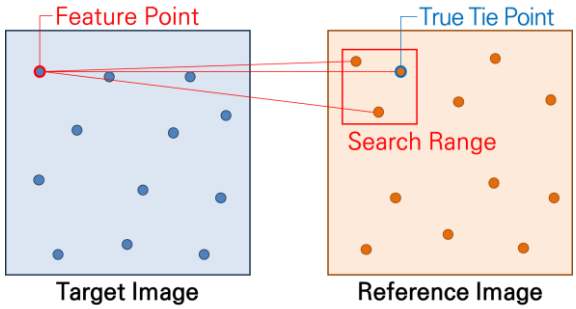

Figure 6. search range constraints in feature matching

2.2.2 Outlier Elimination: Initial tie-points obtained through feature matching inevitably contain outliers. Therefore, we eliminate outliers using RANSAC(Random Sample Consensus). RANSAC is an algorithm used to effectively remove outliers from input data and estimate accurate models. It operates by randomly selecting samples from all data to estimate a model and then evaluating how well the remaining data points support this model to determine the optimal model (Fischler and Bolles, 1981; Kim and Im, 2003). In this study, we use RANSAC to estimate the homography model and, based on this model, assume tie-points with errors exceeding the threshold as outliers and remove them.

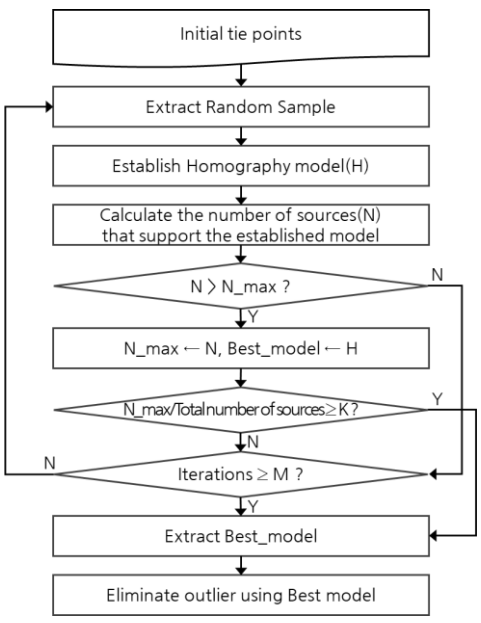

Figure 7. Workflow of RANSAC

2.2.3 Model Estimation and Resampling: Based on the refined tie-points by RANSAC, we estimate the transformation model between the input images. In this study, we apply the Homography model, assuming the images as planes in three-dimensional space. We resample the pixels of the target image to align with the reference image, based on the estimated homography model.

2.3 Multi-Strip Image Mosaicking

Based on the seamline extraction and relative geometric correction techniques, we develop a multi-strip image mosaicking method for KOMPSAT-3A. This method consists of four major steps: strip restoration, strip pair analysis, relative geometric correction and seamline extraction.

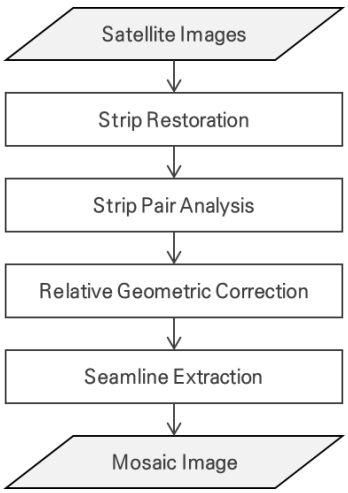

Figure 8. Workflow of multi-strip image mosaicking

In the strip restoration step, we group images along the same strip and mosaicked images along the same image strips. Given that scenes from the same strip of KOMPSAT-3A are acquired with consistent orbit and geometry, we assume there is no relative geometric error. We perform mosaicking solely through seamline extraction without relative geometric correction.

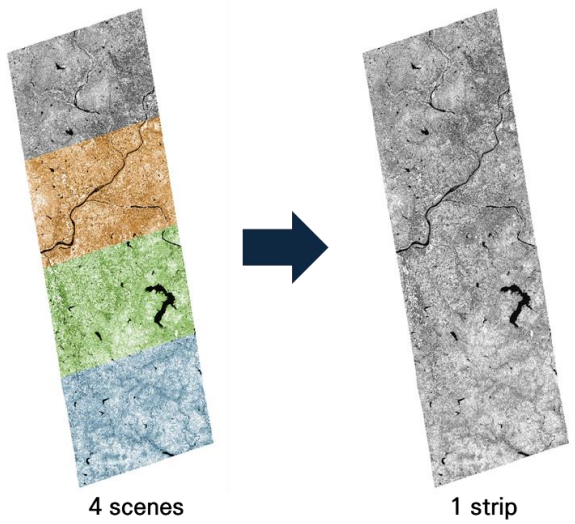

Figure 9. Example of strip restoration

In the second step, we compose strip pairs based on the overlap between strips. The overlap between two strips is calculated using the initial geometric information of the KOMPSAT-3A images. Strips with an overlap exceeding 10% are defined as a pair. The strip having the most pairs is set as the reference strip. We then calculate the shortest path from this reference strip to each of the other strips to compose the final strip pairing.

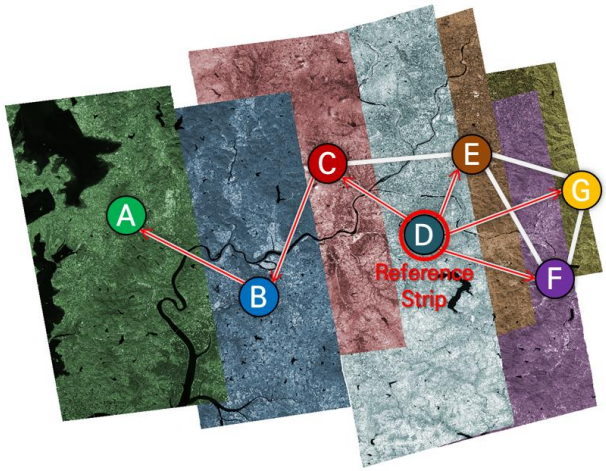

Figure 10. Example of strip pair composition

In the third step, we perform the relative geometric correction between strip pairs. Through this process, all strips are registered based on the reference strip, eliminating the relative geometric errors. Finally, we extract the final seamlines between the corrected image strips and generate the final mosaic image.

3. Experiments and Analysis

3.1 Experiments data

For the experiment, we utilized KOMPSAT-3A L1G data. KOMPSAT-3A, developed by the Korea Aerospace Research Institute (KARI), is a high-resolution optical satellite equipped with an electro-optical camera at a spatial resolution of 55 cm. Level1G is a product that has been orthorectified based on the initial geometric information. Due to the uncorrected distortions in the initial geometric information, significant relative geometric errors can exist between the images. We used KOMPSAT-3A L1G 29 scenes, which were composed of 10 different strips. To analyze the performance of the relative geometric correction, we manually extracted 35 check points across scenes.

Strip	Orbit Num.	Acquisition date	No. of Scene
Strip 1	17156	2018.05.04	4
Strip 2	17564	2018.05.31	3
Strip 3	19332	2018.09.25	2
Strip 4	22022	2019.03.22	3
Strip 5	22430	2019.04.18	3
Strip 6	26208	2019.12.24	3
Strip 7	27281	2020.03.04	2
Strip 8	38389	2022.03.09	3
Strip 9	38661	2022.03.27	3
Strip 10	38782	2022.04.04	3

Table 1. Experiment data

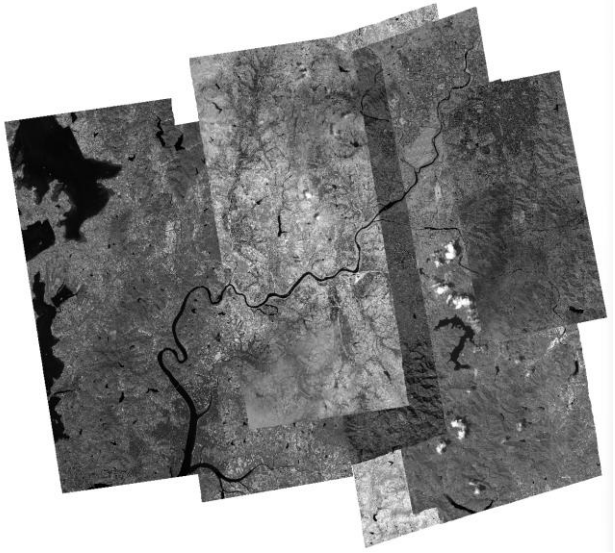

Figure 11. KOMPSAT-3A Image used in experiment

3.2 Experiments Results

We performed the proposed multi-strip image mosaicking using the experiments data and analyzed the results of relative geometric correction and seamline extraction.

Using the experimental dataset, we quantitatively and qualitatively analyzed the results of relative geometric correction for 7 strip pairs. Firstly, we calculated the geometric errors before and after the relative geometric correction based on 35 check points. As shown in Table 2, the results showed that the relative geometric error decreased in all image pairs, confirming a high geometric accuracy with an average error of 1.63 pixels. For Pair #4, the initial relative geometric error was significantly high. After applying the relative geometric correction, the error was successfully reduced to 1.92 pixels. For Pair #5, it was the only case where, even after relative geometric correction, an error greater than 2 pixels was observed. This was attributed to the influence of clouds in the target strip of that pair. We also visually analyzed the results of the relative geometric correction (Table 3). Before the relative geometric correction, mismatches were identified in various objects like roads, buildings, fields, and rivers. However, after the correction, it was confirmed that most of these mismatches had been rectified.

Pair	Reference Strip	Target Strip	Relative Geometric Error (pixels)	
			Before Correction	After Correction
# 1	Strip 8	Strip 1	3.58	0.40
# 2	Strip 8	Strip 2	9.36	1.42
# 3	Strip 8	Strip 3	11.74	2.00
# 4	Strip 8	Strip 6	48.47	1.92
# 5	Strip 8	Strip 7	4.97	2.54
# 6	Strip 8	Strip 9	4.05	1.49
# 7	Strip 8	Strip 10	4.02	1.64
Average	-	-	12.31	1.63

Table 2. relative geometric error analysis

As results of seamline extraction using relative geometric corrected strip, we were able to obtain high-quality seamlines and seamless mosaic image (Figure 12). As shown in Figure 13, the extracted seamlines were following linear features in the images such as roads, rivers, and field boundaries and they minimized geometric distortions and mismatches between the images.

Pair	Before Relative Geometric Correction	After Relative Geometric Correction	Pair	Before Relative Geometric Correction	After Relative Geometric Correction
#1	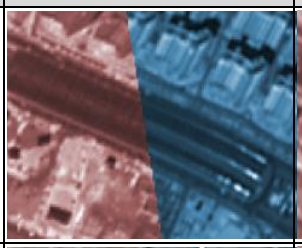	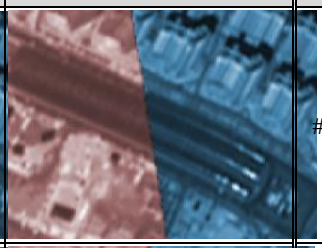	#4		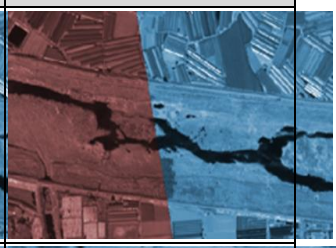
#2			#5	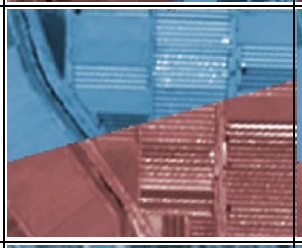	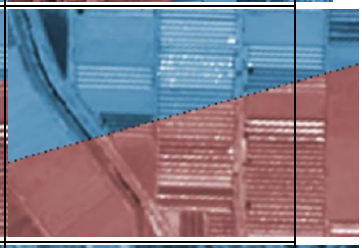
#3	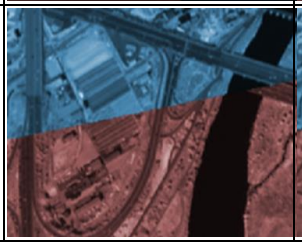	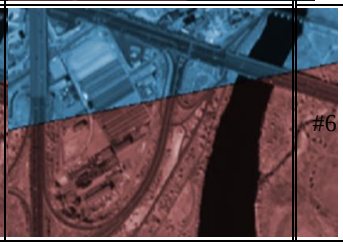	#6		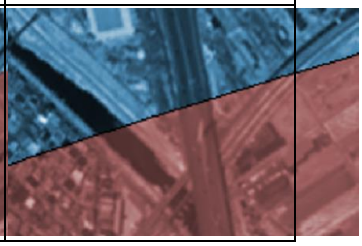

Table 3. Relative geometric correction results

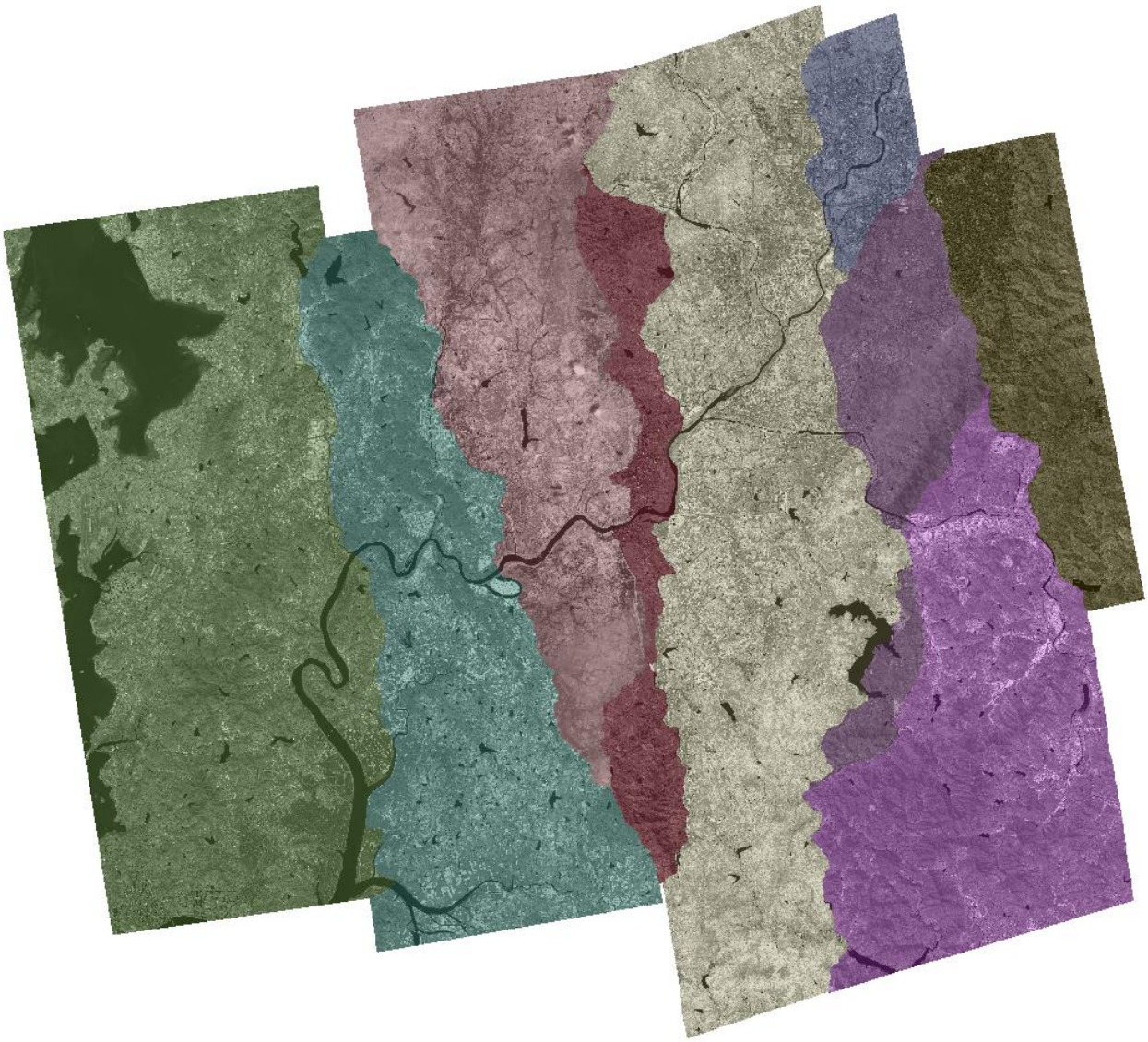

Figure 12. A multi-strip mosaicking result from 29 KOMPSAT-3A images acquired from 10 strips

Figure 13. Examples of extracted seamlines.

4. Conclusion

In this paper, we have presented a seamline extraction and relative geometric correction approach optimized for satellite imagery. Based on this, we achieved accurate and seamless multi-strip image mosaicking for KOMPSAT-3A images. We anticipate this method to enhance the utility of KOMPSAT-3A for extensive area analysis. In our future study, we plan to develop an image mosaicking technique based on block adjustments, instead of pairwiase homography models, for very large region of interest.

Acknowledgements

This work was supported by National Institute of Agricultural Sciences, Rural Development Administration, Republic of Korea, "Research Program for Agricultural Science & Technology Development (Project No. PJ0162342023)" and the “Development of Application Technologies and Supporting System for Microsatellite Constellation” project through the National Research Foundation of Korea (NRF) grant funded by the Korea government (MSIT) (No. 2021M1A3A4A11032019) and the Korea Aerospace Research Institute for providing data used in this study.

References

Milgram, D. L., "Computer Methods for Creating Photomosaics," in IEEE Transactions on Computers, vol. C-24, no. 11, pp. 1113-1119, Nov. 1975, doi: 10.1109/T-C.1975.224142.

Yang, S., Li, L., and Peng, G., "Two-dimensional seam-point searching in digital image mosaicking," Photogrammetric Engineering and Remote Sensing, vol. 55, no. 1, pp. 49-53, 1989.

Afek, Y. and Brand, A., "Mosaicking of orthorectified aerial images," Photogrammetric Engineering and Remote Sensing, vol. 64, no. 2, pp. 115-124, 1998.

Li, L., et al., "Edge-enhanced optimal seamline detection for orthoimage mosaicking," IEEE Geoscience and Remote Sensing Letters, vol. 15, no. 5, pp. 764-768, 2018.

Zhang, Y., et al., "Seamline optimisation for urban aerial ortho-image mosaicking using graph cuts," The Photogrammetric Record, vol. 33, no. 161, pp. 131-147, 2018.

Yuan, S., et al., "Automatic seamline determination for urban image mosaicking based on road probability map from the D-LinkNet neural network," Sensors, vol. 20, no. 7, 1832, 2020.

Kim, H.S., Lee, T.Y., Hur, D.S., Rhee, S.A., and Kim, T., "Automated Geometric Correction of Geostationary Weather Satellite Images," Korean Journal of Remote Sensing, vol. 23, pp. 297–309, 2007.

Kim, H.-G., Son, J.-H., and Kim, T., "Geometric correction for the geostationary ocean color imager from a combination of shoreline matching and frequency matching," Sensors, vol. 18, no. 11, 3599, 2018.

Li, X., et al., "Remote sensing image mosaicking: Achievements and challenges," IEEE Geoscience and Remote Sensing Magazine, vol. 7, no. 4, pp. 8-22, 2019.

Zagrouba, E., Barhoumi, W., and Amri, S., "An efficient image-mosaicing method based on multifeature matching," Machine Vision and Applications, vol. 20, no. 3, pp. 139-162, 2009.

Dijkstra, E. W., "A note on two problems in connexion with graphs," in Edsger Wybe Dijkstra: His Life, Work, and Legacy, pp. 287-290, 2022.

Duplaquet, M.-L., "Building large image mosaics with invisible seam lines," in Visual Information Processing VII, vol. 3387, SPIE, 1998.

Lowe, D. G., "Distinctive image features from scale-invariant keypoints," International Journal of Computer Vision, vol. 60, pp. 91-110, 2004.

Wu, J., et al., "A Comparative Study of SIFT and its Variants," Measurement Science Review, vol. 13, no. 3, pp. 122-131, 2013.

Fischler, M. A. and Bolles, R. C., "Random sample consensus: a paradigm for model fitting with applications to image analysis and automated cartography," Communications of the ACM, vol. 24, no. 6, pp. 381-395, 1981.

Kim, T. and Im, Y.-J., "Automatic satellite image registration by combination of matching and random sample consensus," IEEE Transactions on Geoscience and Remote Sensing, vol. 41, no. 5, pp. 1111-1117, 2003.